



Spin-Hall effect due to the bulk states of topological insulators: Extrinsic contribution to the proper spin current

James H. Cullen  and Dimitrie Culcer *School of Physics, The University of New South Wales, Sydney 2052, Australia*

(Received 10 September 2023; revised 20 November 2023; accepted 4 December 2023; published 18 December 2023)

The substantial amount of recent research into spin torques has been accompanied by a revival of interest in the spin-Hall effect. This effect contributes to the spin torque in many materials, including topological insulator/ferromagnet devices, Weyl semimetals, and van der Waals heterostructures. In general, the relative sizes of competing spin torque mechanisms remain poorly understood. Whereas a consensus is beginning to emerge on the evaluation of the proper spin current, the role of extrinsic disorder mechanisms in the spin-Hall effect has not been clarified. In this work, we present a comprehensive calculation of the *extrinsic* spin-Hall effect while focusing on the bulk states of topological insulators as a prototype system and employing a fully quantum-mechanical formalism to calculate the proper spin current. Our calculation of the proper spin current employs a 4×4 $\mathbf{k} \cdot \mathbf{p}$ Hamiltonian describing the bulk states of topological insulators. At the same time, we provide a qualitative explanation of the proper spin currents calculated based on an effective 2×2 Hamiltonian obtained via a Schrieffer-Wolf transformation. We find that the extrinsic contribution to the proper spin current, driven by side jump, skew scattering, and related mechanisms, is of a comparable magnitude to the intrinsic contribution, making it vital to take such disorder effects into account when seeking to understand experiments. Among the scattering effects considered, side jump scattering is the primary contributor to the extrinsic spin-Hall effect. The total spin conductivity calculated here is too small to explain experimentally measured spin torques, hence we expect the spin-Hall effect to make a negligible contribution to the spin torque in topological insulator structures.

DOI: [10.1103/PhysRevB.108.245418](https://doi.org/10.1103/PhysRevB.108.245418)

I. INTRODUCTION

The spin-Hall effect (SHE), the generation of a transverse spin current in response to an applied electric field, has witnessed a surge of renewed interest in recent years due to its relevance to spin torques, which provide a promising avenue towards electrical control of magnetic degrees of freedom [1–6]. Following its prediction [7–11], the SHE has been observed in semiconductors [12,13] and metals [14–23]. Recently, it has been studied in more exotic materials such as topological insulators, Weyl semimetals [24,25], and van der Waals heterostructures [26–33]. Spin torque devices that utilize the spin Hall effect do this by generating spin currents in a material with spin-orbit coupling which flow into an adjacent magnetic material in which the polarized spins exert a torque on the magnetization. The inverse spin Hall effect has also received considerable research interest [34–41], as it has its own spintronic applications in spin-to-charge conversion. While spin currents of intrinsic origin have received most theoretical attention [42–45], the need persists for a more profound understanding of extrinsic spin currents, which form the subject of this work.

The difficulty in theoretically studying the spin-Hall effect lies in the definition of the spin current. The intuitive and conventional definition of the spin current is the product of the spin and velocity operators [46–55]. However, the generation of a spin current generally requires spin-orbit coupling, which causes spin precession and hence nonconservation.

This makes the conventional definition meaningless in most contexts of interest. One way to address this is to circumvent the spin current altogether by calculating directly the spin density and/or spin accumulation [56–59]. However, there are many systems where the spin current itself is the quantity of interest, including magnetic systems with sizable spin-Hall torques, discussed below. The charge current generated in the inverse SHE is the Onsager inverse of the spin current in the SHE [45], and hence employing the correct physical definition of the spin current is also important for understanding this effect. To evaluate the spin-Hall effect in spin-orbit coupled systems, one needs to evaluate the proper spin current, which takes into account the torque dipole arising from spin precession [45,60–67]. The torque dipole is notoriously difficult to evaluate for Bloch electrons, and, until recently, available theories only provided results for simple two-dimensional (2D) effective spin-1/2 models, with the spin primarily in the plane. However, there have been new developments in the understanding of the SHE and the proper spin current. Two recent theories have brought to light the relationship between the intrinsic proper spin current and the underlying topological structure of the Hilbert space, with very similar results [44,45]. A quantum-mechanical study determined the intrinsic contribution to the proper spin current and SHE, relating the intrinsic proper spin current to the interband matrix elements of the Berry connection [44]. The results are broadly in agreement with the evolving semiclassical understanding of the SHE [45], in which the intrinsic proper spin current is

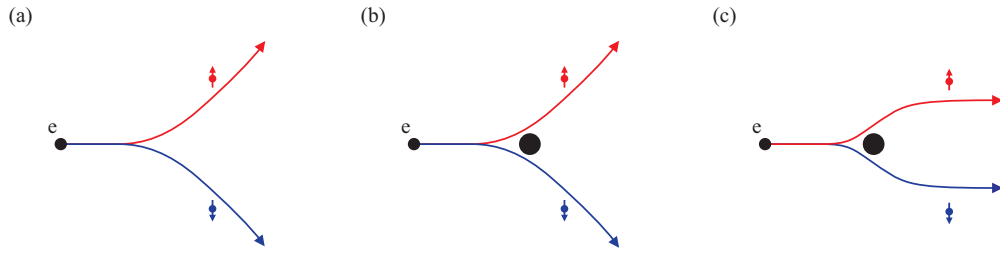


FIG. 1. Spin-Hall effect mechanisms: (a) Intrinsic mechanism, electrons with opposite spin experience opposite spin-orbit fields due to the band structure of the material, and hence they tend to follow different trajectories. (b) Skew scattering, electrons scattering off of impurities in the material will scatter in different directions depending on their spin. (c) Side jump, electrons scattering off of impurities are displaced spatially and the direction will depend on their spin; the net effect of these displacements can generate a current. These scattering effects can occur due to the spin-orbit coupling of the impurity or due to the interplay between the impurity potential and the materials intrinsic spin-orbit coupling.

expressed in terms of the Berry curvature. The semiclassical study also considered nonuniform systems, including first-order spatial gradients, which is necessary for spin currents in equilibrium [45].

A complete description of the spin Hall effect must necessarily include extrinsic mechanisms due to impurity scattering. Scattering introduces sizable transport effects that are independent of the disorder strength, making them indistinguishable from intrinsic mechanisms. This has been studied in depth using the conventional definition of the spin current [68–73], and it is also known to occur in the anomalous Hall effect [74–76]. Extrinsic effects on the proper spin current have been studied in the past in Ref. [68], which presented a formula for the proper spin current that included disorder effects. This work clearly showed that the inclusion of disorder is vital for an accurate calculation of the proper spin current, as it showed that disorder effects can sometimes be the dominant contribution to the proper spin current. The complex semiclassical approach of Ref. [68] requires the use of fictitious electric and magnetic fields with respect to the wave packet center of mass, and it does not directly relate to topological quantities. Furthermore, although the approach can be applied more generally, the formula presented is restricted to specific 2D spin-1/2 systems with the spin lying in the plane. This calls for a general, systematic theory of disorder in the context of the proper spin current and the SHE.

In light of the above, in this paper we develop a fully quantum-mechanical formalism for the calculation of proper spin currents of extrinsic origin, including skew scattering and side jump. This work aims to (i) provide a general blueprint for calculating the full spin current in the presence of disorder, and (ii) apply this method to calculate the full spin Hall effect due to the bulk states of 3D topological insulators, focusing on the disorder contributions. We determine the extrinsic spin currents up to zeroth order in the scattering time τ , which we take to be a measure of the disorder strength. We consider the effects of a scalar disorder potential combined with band-structure spin-orbit coupling, leading to skew scattering and side jump, with the latter incorporating an electric field correction to the scattering term [78–81]. Pedagogical diagrams of these mechanisms are shown in Fig. 1. The spin current contributions from these two mechanisms appear to zeroth order in the scattering time. They are independent of disorder strength and appear due to the disorder-independent part of

the nonequilibrium density matrix $\rho_E^{(0)}$. Hence, these extrinsic contributions to the spin current compete with the intrinsic contributions [79,81], which by definition are independent of the disorder strength. It is crucial to consider disorder effects on the proper spin current: not only is this the only physically meaningful definition, but, as the study of the intrinsic case shows, many of the conventional spin current terms are exactly canceled by the torque dipole correction [44], and it is natural to expect similar cancellations in the extrinsic contributions.

We consider, as a prototype system, the bulk states of topological insulators (TIs). This choice is motivated by the observation that topological insulators are excellent candidates for building spin torque devices due to their high charge to spin conversion efficiency. Spin torques are especially strong in topological insulators [82–94], and large spin torques have been demonstrated experimentally in a plethora of ferromagnet (ferrimagnet)/TI heterostructures [95–110], including room-temperature magnetization switching [111–114]. The extent to which the spin-Hall effect contributes to the spin torque has yet to be conclusively settled [83,97,105,115], and a full account of the spin-Hall effect cannot be given without considering the extrinsic contribution to the physical spin current.

Hence, for concreteness, after introducing the general formalism for calculating the proper spin current in the presence of disorder, we determine the linear response of the TI bulk density matrix to an electric field in a system with short-ranged nonmagnetic impurities. We then formulate an expression for the extrinsic proper spin current using the same approach that was used in Ref. [44] for the intrinsic case. The main results we present are as follows: (i) The extrinsic spin-Hall effect in TIs is of a similar magnitude to the intrinsic spin-Hall effect, as shown in Fig. 2, which may be regarded as a summary of the central results of this work; (ii) the largest component of the extrinsic spin current, primarily driven by side jump scattering, should generate a fieldlike spin torque; (iii) the size of the spin currents generated by the spin-Hall effect in TIs should have a negligible contribution on the total spin torque. As Fig. 2 shows, the spin conductivities due to the SHE are of the order $10^3(\hbar/2e)\Omega^{-1}m^{-1}$, which is one to two orders of magnitude smaller than the spin conductivities reported in experiment [95,111,112,114]. Hence, the only potentially sizable bulk state contribution to the TI spin torque

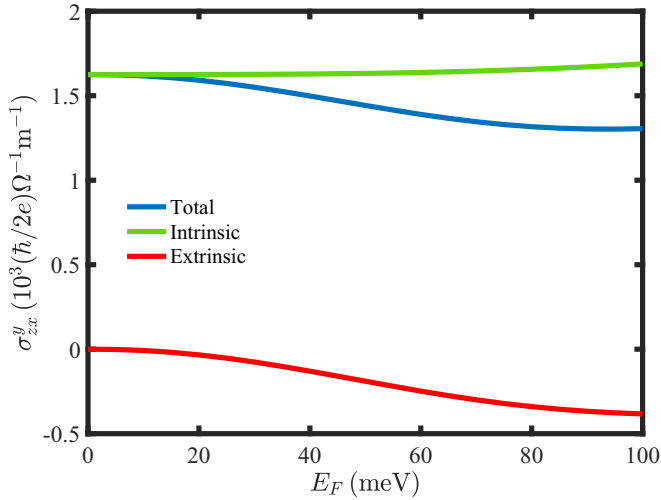


FIG. 2. The spin-Hall conductivity σ_{zx}^y vs the Fermi energy E_F for the TI bulk states in Bi_2Se_3 with Zeeman field $\mathbf{m} \parallel \hat{z}$ and $|\mathbf{m}| = 10 \mu\text{eV}$ (Bi_2Se_3 parameters from Ref. [77]).

is the spin transfer torque, introduced in Ref. [116]. We note, at the same time, that the expression we present for the spin current is general and can be applied in further studies to other materials of interest.

This paper is organized as follows: first in Secs. II and III we present the model Hamiltonian and linear-response formalism based on the density matrix. Next we discuss the calculation of the proper spin current, and we present a general formula for its evaluation. Then in Sec. IV we present our results for the extrinsic spin conductivity in topological insulators, focusing on Bi_2Se_3 for concreteness. We show that different components of the spin current have different dependencies on the impurity strength and Zeeman field. In Sec. V we discuss the role of the extrinsic and intrinsic spin Hall effect in topological insulator spin torques and potential ways to measure the extrinsic spin-Hall effect. Lastly, we discuss the applicability of our proper spin current calculation to other systems.

II. MODEL HAMILTONIAN

Bulk TI states are described by the Hamiltonian $H_0 = \epsilon_{\mathbf{k}} + H_{\text{so}} + U + e\mathbf{E} \cdot \mathbf{r}$, where $\epsilon_{\mathbf{k}} = C_0 + C_1 k_z^2 + C_2 k_{\parallel}^2$, the spin-orbit Hamiltonian H_{so} is given by Ref. [77], U is the disorder contribution, \mathbf{r} is the position operator, and $e\mathbf{E} \cdot \mathbf{r}$ is the electric potential. The disorder contribution is calculated using the Born approximation, and the electric potential is treated perturbatively. In the basis $\{1/2, -1/2, 1/2, -1/2\}$, the spin-orbit Hamiltonian is

$$H_{\text{so}} = \begin{pmatrix} -\mathcal{M} + m_z & m_- & \mathcal{B}k_z & \mathcal{A}k_- \\ m_+ & -\mathcal{M} - m_z & \mathcal{A}k_+ & -\mathcal{B}k_z \\ \mathcal{B}k_z & \mathcal{A}k_- & \mathcal{M} + m_z & m_- \\ \mathcal{A}k_+ & -\mathcal{B}k_z & m_+ & \mathcal{M} - m_z \end{pmatrix}, \quad (1)$$

with $\mathcal{M} = M_0 + M_1 k_z^2 + M_2 k_{\parallel}^2$, $\mathcal{A} = A_0 + A_2 k_{\parallel}^2$, $\mathcal{B} = B_0 + B_2 k_z^2$, $k_{\parallel}^2 = k_x^2 + k_y^2$, $k_{\pm} = k_x \pm ik_y$, and $m_{\pm} = m_x \pm im_y$. In our Hamiltonian, we include a small Zeeman field \mathbf{m} to

remove spin degeneracy; for most of our calculations, we set it to be $10 \mu\text{eV}$. It can be thought of as spin splitting due to an applied external magnetic field, as one is often used in spin torque experiments [6]. For most of the calculation, we have ignored the hexagonal warping terms due to the added complexity. However, their effects have been calculated and are discussed in Sec. IV.

This model is only accurate near the band center and is valid in the regime $k < 4 \times 10^8 \text{ m}^{-1}$. We use this $\mathbf{k} \cdot \mathbf{p}$ Hamiltonian here despite its limitations as it allows us to apply our transport formalism to the problem. Our approach has an advantage over other numerical models and methods that struggle to properly treat disorder.

III. LINEAR RESPONSE

We use a kinetic equation formalism to calculate the linear response of the bulk states to an electric field \mathbf{E} , starting from the quantum Liouville equation as described in Refs. [78,81,117]. This transport formalism can be thought of as the quantum analog of the Boltzmann equation. The linear response of the bulk states is characterized by the following kinetic equation:

$$\frac{\partial \langle \rho_E \rangle}{\partial t} + \frac{i}{\hbar} [H_0, \langle \rho_E \rangle] + \hat{J}_0(\langle \rho_E \rangle) = \frac{e\mathbf{E}}{\hbar} \cdot \frac{D\langle \rho_0 \rangle}{D\mathbf{k}}, \quad (2)$$

where \mathbf{k} is the wave vector, $\langle \rho_0 \rangle$ is the equilibrium density matrix, $\langle \rho_E \rangle$ is the nonequilibrium density matrix to first order in the electric field, and \hat{J} contains the disorder contribution. The equilibrium density matrix is simply the Fermi-Dirac distribution. Here $\langle \rho \rangle$ represents the disorder-averaged density matrix. The differential $D/D\mathbf{k}$ is the covariant derivative defined by $D\hat{O}/D\mathbf{k} = d\hat{O}/d\mathbf{k} - i[\mathcal{R}, \hat{O}]$, where \mathcal{R} is the Berry connection.

To solve this kinetic equation, we break the density matrix $\langle \rho_E \rangle$ up into two components: n_E , a band diagonal part, and S_E , a band off-diagonal part. In the steady-state limit, the kinetic equation for the diagonal part simplifies greatly, and the solution can be found by solving the equation

$$[\hat{J}_0(n_E)]_{mn} = \frac{e\mathbf{E}}{\hbar} \cdot \frac{\partial f_k^n}{\partial \mathbf{k}}. \quad (3)$$

Carrying out the time integral for the off-diagonal part gives

$$S_{E, nm} = -i\hbar \frac{e\mathbf{E} \cdot \mathcal{R}_{nm}(f_k^n - f_k^m) - [\hat{J}_0(n_E)]_{nm}}{\epsilon_k^n - \epsilon_k^m}, \quad (4)$$

where ϵ_k^n is the energy of the eigenstate in band n with wave vector \mathbf{k} . The first part of (4) is purely intrinsic and will be ignored in this calculation; the spin current due to this term was studied in Ref. [44]. The disorder contribution \hat{J} is calculated in the Born approximation. The Born approximation scattering term is

$$J(\hat{f}) = \frac{1}{\hbar^2} \int_0^\infty dt' \langle e^{-nt'} [\hat{U}, e^{-i\hat{H}t'/\hbar} [\hat{U}, \hat{f}] e^{i\hat{H}t'/\hbar}] \rangle_{\mathbf{k}\mathbf{k}}. \quad (5)$$

Here we consider short-ranged scalar disorder of the form $U_i = U_0 \delta(\mathbf{r}_i - \mathbf{r})$, where the impurities are enumerated by the index i . We are concerned with the disorder-averaged density matrix and kinetic equation, so this index i has been summed over. The way in which this scattering integral is calculated is

outlined in Ref. [117]. Calculating the scattering integral (5) and solving (3) will give the band diagonal response to order -1 in the impurity density. Substituting this solution into (4) will give the extrinsic off-diagonal density matrix to zeroth order in the impurity density.

To find the diagonal part of the nonequilibrium density matrix to zeroth order in the impurity density, we need to include some extra corrections to the scattering term. The band-diagonal kinetic equation to zeroth order in the impurity density is

$$\frac{\partial n_E^0}{\partial t} + \frac{i}{\hbar} [H_0, n_E^0] + \hat{J}_0(n_E^0) = -\hat{J}_E(\langle \rho_0 \rangle) - \hat{J}_{sk}(n_E^{-1}), \quad (6)$$

where \hat{J}_E is an electric field correction to the scattering term [78], and \hat{J}_{sk} is the scattering term found by substituting (4) back into the band-diagonal part of the scattering integral (5). In semiclassical calculations, \hat{J}_E is considered to be part of side-jump scattering and \hat{J}_{sk} part of skew-scattering [78,80,81]. We find that these scattering terms are crucial for a proper calculation of the extrinsic spin current.

The general definition of the proper spin current is $\hat{\mathcal{J}}_j^i = d(\hat{r}_j \hat{s}_i)/dt$. The regularly used conventional spin current $J_j^i = 1/2\{s_i, v_j\}$ fails to account for the absence of spin conservation in materials with spin orbit coupling. As has been shown in a recent paper, the proper intrinsic spin current can be captured by the following equation [44]:

$$\mathcal{J}_{jl}^i = \sum_k \left[\frac{eE_l \hat{l}}{\hbar} \times \sum_m \Sigma_m^i f_m \right]_j, \quad (7)$$

where Σ is a topological quantity related to the Berry connection and spin operator. This formula only captures intrinsic spin currents and does not account for disorder contributions. However, disorder contributions can be straightforwardly calculated using the same methodology used in Ref. [44]. Here we will evaluate these extra contributions.

The proper spin current can be broken up into two parts:

(i) The conventional spin current $\{s_i, v_j\}$, where the extrinsic terms due to the conventional spin current are

$$J_{jl}^i = \sum_{m,k} \frac{s_{mm}^i n_m^{E_l}}{\hbar} \frac{\partial \epsilon_m}{\partial k_j} - \frac{s_{mm}^i}{2} \{ \mathcal{R}_j, [\hat{J}_0(n_{E_l})]_{od} \}_{mm}. \quad (8)$$

(ii) The torque dipole correction $\{\partial s_i / \partial t, \hat{r}_j\}$.

To evaluate the torque dipole in the proper spin current, we must allow the density matrix to have terms that are off-diagonal in the wave vector k . To do this, we expand the density matrix $\rho_{kk'}$ perturbatively in terms of a small off-diagonal wave vector \mathcal{Q} , such that $\mathbf{k} \equiv \mathbf{q}_+ = \mathbf{q} + \mathcal{Q}/2$ and $\mathbf{k}' \equiv \mathbf{q}_- = \mathbf{q} - \mathcal{Q}/2$. Using this transformation, we can reformulate our kinetic equation. This will give successive equations each of increasing order in the perturbation \mathcal{Q} ; the zeroth-order equation is simply (2). The kinetic equation to first order in \mathcal{Q} is

$$\frac{\partial \rho_{q\mathcal{Q}}}{\partial t} + \frac{i}{\hbar} [H_{0q}, \rho_{q\mathcal{Q}}] + \hat{J}_0(\rho_{q\mathcal{Q}}) = -\frac{i\mathcal{Q}}{2\hbar} \cdot \left\{ \frac{DH_{0q}}{Dq}, \rho_q \right\}, \quad (9)$$

where ρ_q is simply the solution to (2) and $\rho_{q\mathcal{Q}}$ is the density matrix to first order in \mathcal{Q} . This kinetic equation is solved in an identical manner to (2), as the scattering term to linear order

in \mathcal{Q} is identical to the scattering term diagonal in wave vector. Due to the form of the torque dipole operator, only solutions to the first order in \mathcal{Q} are required for the proper spin current calculation.

The extrinsic term from the torque dipole contribution is

$$I_{jl}^i = \text{Tr } t_{i,q} \left(\frac{\partial S_{q\mathcal{Q}, E_l}}{\partial Q_j} \right)_{\mathcal{Q} \rightarrow 0}, \quad (10)$$

where $t_i = i/\hbar[H_0, s_i]$, and the part of $S_{q\mathcal{Q}}$ that contributes to the spin current is

$$S_{q\mathcal{Q}}^{mn} = -i\hbar \frac{J_{mn}(n_{q\mathcal{Q}})}{\epsilon_m - \epsilon_n}. \quad (11)$$

The terms in (8) and (10) together give the extrinsic proper spin current. Note that the kinetic equations used in this derivation assume that the system is in the weak scattering limit [117]. Hence, this formula can be used generally to calculate extrinsic spin currents in the weak scattering limit for any system that can be described by a single-particle Hamiltonian, in this work we focus on spin currents in topological insulators.

IV. RESULTS

We solved Eqs. (2), (6), and (9) numerically to find the linear response of the TI bulk states to an electric field, and we calculated the induced spin currents flowing out-of-plane $\parallel \hat{z}$. We calculated the scattering term \hat{J}_0 by first integrating the scattering out, then the scattering in was calculated iteratively until convergence was reached. Further details on this part of the calculation can be found in the Supplemental Material [118].

We calculated the spin conductivities σ_{zx}^i , where $i = x, y, z$. This means that we have a spin current flowing in \hat{z} of spins aligned along \hat{i} in response to an electric field along \hat{x} . These are the spin conductivities relevant to spin torques, as we are concerned with spins flowing from the TI into the interface with the magnetic material. For the following discussion, we set the Zeeman field $\mathbf{m} \parallel \hat{z}$. We discuss results for other Zeeman field orientations later. We found \mathcal{J}_{zx}^z to be exactly 0. However, we found spin currents \mathcal{J}_{zx}^x and \mathcal{J}_{zx}^y to be nonzero.

A. Extrinsic contributions to the TI SHE

The primary contributions to the spin current \mathcal{J}_{zx}^y originate from the electric field correction to the scattering as well as the band-structure skew scattering. Interestingly, it has recently been shown that these same mechanisms are also important for the surface-state torque [119,120]. We find that there is also a contribution from the extrinsic off-diagonal elements of the density matrix S_E , however this contribution is of a negligible magnitude. This means that the primary contribution to this spin-Hall current comes from n_E^0 , hence the size of this spin current should be independent of the impurity density.

The spin current \mathcal{J}_{zx}^x is due to the band diagonal part of the density matrix $n_E^{(-1)}$, and it can be of a similar order of magnitude to the intrinsic spin current. This spin current does not have any contributions from the electric field scattering, skew scattering, band off-diagonal elements, or the torque dipole correction. This means that this spin current is linear in

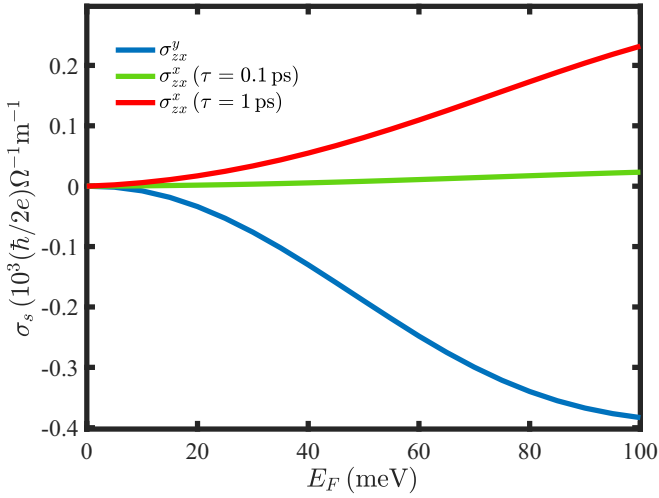


FIG. 3. The total extrinsic spin-Hall conductivity σ_s vs the Fermi energy E_F for the TI bulk states in Bi_2Se_3 with Zeeman field $\mathbf{m} \parallel \hat{z}$ and $|m| = 10 \mu\text{eV}$ (Bi_2Se_3 parameters from Ref. [77]).

the scattering time and can be enhanced in clean samples with a lower impurity density. Estimations based on experimental results of the bulk conductivity [121] indicate that Bi_2Se_3 has a scattering time of order 0.1 ps. So we chose numbers for the impurity density and scattering potential such that we have a scattering time of the same order of magnitude. Calculations with larger scattering times have also been included to demonstrate the dependence of the spin current on the impurity density. Furthermore, the spin current \mathcal{J}_{zx}^x is linear in the Zeeman energy, and for a Zeeman energy of $m_z = 1 \text{ meV}$ and scattering time $\tau = 0.1 \text{ ps}$ its magnitude is twice the value of the spin current \mathcal{J}_{zx}^y . This shows that it is also possible to enhance the extrinsic spin-Hall effect in magnetized TIs.

We find that in the TI bulk, the spin current due to the torque dipole correction (10) is zero for both spin currents \mathcal{J}_{zx}^x and \mathcal{J}_{zx}^y . The spin current from the conventional spin current (8) is the only contribution to the extrinsic proper spin current. However, even in this case it is crucial to use the proper spin current and not the conventional spin current as most of the contributions from the torque dipole correction exactly cancel terms in the conventional spin current [44]. Further details on these cancellations can be found in the Supplemental Material [118].

We note that the model Hamiltonian is accurate up to a Fermi energy of around 20 meV and remains reasonably accurate up until 40 meV [77]. Our results beyond this point should be regarded as approximate: they are included here since experimentally the chemical potential of Bi_2Se_3 will often be on the order of 100 meV [122–124].

In Fig. 3 we plot the total extrinsic spin conductivity versus the Fermi energy. We set the zero of energy at the conduction-band minimum. The plot shows that the magnitude of the extrinsic spin conductivities tends to increase monotonically with the Fermi energy. It also shows that the extrinsic spin conductivities are of a comparable magnitude to the intrinsic spin conductivity calculated in Ref. [44]. The spin conductivity σ_{zx}^x is plotted for two different scattering times, $\tau = 0.1, 1 \text{ ps}$. Note, the scattering time is dependent on the Fermi

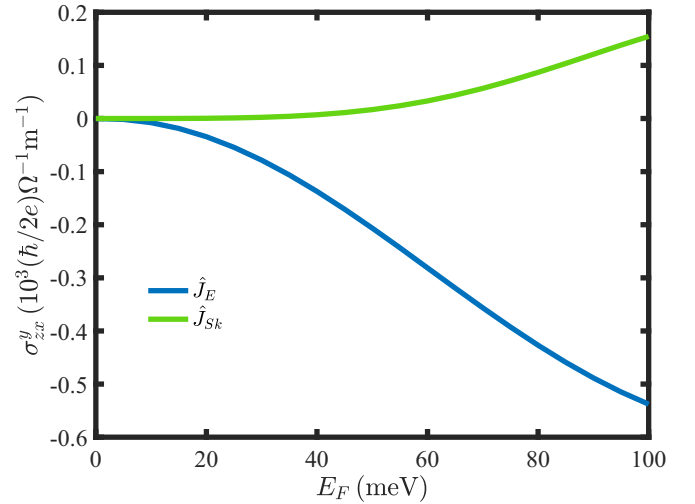


FIG. 4. The extrinsic spin-Hall conductivity σ_{zx}^y vs the Fermi energy E_F for the TI bulk states due to skew scattering and electric field scattering in Bi_2Se_3 with Zeeman field $\mathbf{m} \parallel \hat{z}$ and $|m| = 10 \mu\text{eV}$ (Bi_2Se_3 parameters from Ref. [77]).

energy, and these τ numbers represent the scattering time at $E_F = 50 \text{ meV}$. Since we expect the scattering time to be on the order of magnitude $\tau \sim 0.1 \text{ ps}$, we expect the spin current \mathcal{J}_{zx}^x to be of a negligible order of magnitude compared to \mathcal{J}_{zx}^y . However, we do comment that in very clean samples this may not be the case.

Figure 4 shows the spin conductivity σ_{zx}^y due to the first term in (8) from the electric field and skew scattering terms. In this figure, we can see that the electric field correction gives the largest contribution to the extrinsic spin current, with the spin current due to skew scattering being roughly an order of magnitude smaller than it is at lower Fermi energies, and growing to be about one-third the size of it at 100 meV. Each contribution has an opposite sign and hence they combine destructively when calculating the total spin current.

B. Analysis of extrinsic TI spin currents

We find the direction of the Zeeman field to significantly effect the magnitude and direction of extrinsic spin currents. This is due to the coupling of the Zeeman terms to spin-orbit terms in our Hamiltonian. As shown in Ref. [116], the conduction band will have an effective spin-orbit field of $H_c = \hbar/2 \boldsymbol{\sigma} \cdot \boldsymbol{\Omega} \equiv \hbar/2 (\sigma_z \Omega_z + \sigma_+ \Omega_- + \sigma_- \Omega_+)$, where $\sigma_{\pm} = (\sigma_x \pm i\sigma_y)/2$, $\Omega_z = -(\mathcal{A}^2 k_{\parallel}^2 / \hbar \mathcal{M}^2) m_z + (\mathcal{A} \mathcal{B} k_z / \hbar \mathcal{M}^2) \mathbf{k}_{\parallel} \cdot \mathbf{m}_{\parallel}$, and $\Omega_{\pm} = (\mathcal{A} \mathcal{B} k_{\pm} / \hbar \mathcal{M}^2) m_z - (\mathcal{B}^2 k_z^2 / \hbar \mathcal{M}^2) m_{\pm} + (\mathcal{A}^2 k_{\mp} / \hbar \mathcal{M}^2) (\mathbf{k} \times \mathbf{m})_z$. We can see how this directly relates to our spin currents that are linear in the scattering time. For a Zeeman field $\parallel \hat{z}$ we have a spin current \mathcal{J}_{zx}^x that can be directly related to the term $(\mathcal{A} \mathcal{B} k_z k_x / \hbar \mathcal{M}^2) m_z \sigma_x$ in the spin-orbit field. Furthermore, for a rotated Zeeman field aligned $\parallel \hat{x}$ we find the spin current linear in the Zeeman energy to have the spin rotated such that we get a spin current of identical magnitude \mathcal{J}_{zx}^x , which can be related to the term $(\mathcal{A} \mathcal{B} k_z k_x / \hbar \mathcal{M}^2) m_x \sigma_z$. For a Zeeman field $\parallel \hat{y}$ there will be no spin current that is linear in the scattering

TABLE I. The zero and nonzero spin currents in the TI bulk for different Zeeman field orientations.

	$m \parallel \hat{x}$	$m \parallel \hat{y}$	$m \parallel \hat{z}$
σ_{zx}^x	×	×	✓
σ_{zx}^y	✓	✓	✓
σ_{zx}^z	✓	✓	×

time. This is consistent with the above analysis, as there are no spin orbit terms with m_y, k_x , and k_z .

For the spin currents independent of the scattering time, we find that although they are largely independent of the magnitude of the Zeeman field, they are dependent on the direction of the Zeeman field. The scattering time-independent spin currents can again be described using the effective spin-orbit Hamiltonian. However, it requires a more detailed analysis than was used in the previous paragraph, with reference to the Berry connection and the derivative of the scattering matrix elements, as these are the quantities that appear in the electric field correction to the scattering term \hat{J}_E . In the following analysis, we consider the electric field to be $\parallel \hat{x}$ and the scattering time-independent component of the band diagonal nonequilibrium density matrix $n_E \propto \mathcal{R}_x, \nabla_{k_x} U_{k'k}$. For a Zeeman field $\parallel \hat{x}$, the band diagonal component of the Berry connection \mathcal{R}_x contains a term $(\mathcal{A}^3 \mathcal{B} k_x k_y k_z / 4\mathcal{M}^4) \sigma_z$, and the band diagonal component of the spin operator is $s_{y,d} = (\hbar \mathcal{A}^2 k_x k_y / 4\mathcal{M}^2) \sigma_z$. The band diagonal velocity operator v_z has a factor $\propto k_z \mathbb{I}$. Hence, it is clear that the trace $\text{Tr}[s_{y,d} n_E v_z]$ will be nonzero and that there is spin current \mathcal{J}_{zx, m_x}^y that is third order in the spin-orbit field $\propto |\Omega|^3$. When the Zeeman field is aligned $\parallel \hat{y}$, the band diagonal component of the Berry connection \mathcal{R}_x contains a correction of the form $-(\mathcal{A} \mathcal{B} k_z / 2\mathcal{M}^2) \sigma_z$. This correction to the Berry connection is due to the Schrieffer-Wolf transform that was used to obtain the effective 2×2 Hamiltonian. The leading term in the band diagonal component of the spin operator s_y is $(\hbar/2) \sigma_z$. Hence, the product of these terms with the velocity operator will yield a nonzero spin current \mathcal{J}_{zx, m_y}^y that is first order in the spin-orbit field $\propto |\Omega|$. When the Zeeman field is aligned $\parallel \hat{z}$, the band diagonal component of the Berry connection \mathcal{R}_x contains the term $(-k_y/k_{\parallel}^2 + \mathcal{A}^2 k_y / 2\mathcal{M}^2) \sigma_z$. Interestingly, $\nabla_{k_x} U_{k'k}$ will also yield a term $(k_y/k_{\parallel}^2) \sigma_z$ that will exactly cancel with the first term from the Berry connection. The band diagonal component of the spin operator is $s_{y,d} = (\hbar \mathcal{A} \mathcal{B} k_y k_z / 4\mathcal{M}^2) \sigma_z$. Hence, the product of these terms with the velocity operator will yield a nonzero spin current \mathcal{J}_{zx, m_z}^y that is second order in the spin-orbit field $\propto |\Omega|^2$. Thus, for each of the three orientations of the Zeeman field considered, we find that the spin current \mathcal{J}_{zx}^y will be of a different order in the spin-orbit field.

A summary of the zero and nonzero spin currents can be found in Table I. As is shown in this table, there is an additional nonzero spin current \mathcal{J}_{zx}^z for a Zeeman field aligned $\parallel \hat{y}$. This spin current is independent of disorder strength, and its size is around three orders of magnitude smaller than the other spin currents we have calculated. We find that the magnitude of this spin current is linear in the Zeeman energy. To describe this spin current, we must again refer to the Berry connection and spin operators in the effective spin-

 TABLE II. Extrinsic spin conductivities for Bi_2Se_3 , Bi_2Te_3 , and Sb_2Te_3 , calculated for Fermi energy $E_F = 50$ meV, scattering time $\tau = 0.1$ ps, and Zeeman field $m \parallel \hat{z}$ with $|m| = 10$ μeV (material parameters from Ref. [77]).

	Bi_2Se_3	Bi_2Te_3	Sb_2Te_3
$\sigma_{zx}^x (\hbar/2e) \Omega^{-1} \text{m}^{-1}$	8.0	1.3	-0.15
$\sigma_{zx}^y (\hbar/2e) \Omega^{-1} \text{m}^{-1}$	-189.6	-50.9	-21.0

orbit Hamiltonian. The Berry connection \mathcal{R}_x will contain a component $(\mathcal{A}^2 k_y / 2\mathcal{M}^2) \mathbb{I}$. The spin operator s_z will contain a component $(\mathcal{A} \mathcal{B} k_y k_z / 2\mathcal{M}^3) m_y \mathbb{I}$. This term is a correction due to the rotation of the spin operator s_z by the Schrieffer-Wolf transform. These terms will yield a spin current \mathcal{J}_{zx}^z that is to second order in the spin-orbit field $\propto |\Omega|^2$. However, this spin current \mathcal{J}_{zx}^z has a factor of m_y / \mathcal{M} , which is the ratio of the Zeeman splitting to the band gap. Due to this additional factor, this spin current will be negligible in most cases.

The model Hamiltonian we used can also describe Bi_2Te_3 and Sb_2Te_3 . A comparison of the extrinsic spin-Hall conductivities of each material can be found in Table II. These results show that, of these three materials Bi_2Se_3 should have the largest extrinsic spin-Hall effect.

C. Hexagonal warping

Up to this point, our calculations have ignored the hexagonal warping terms that appear in topological insulators. These extra warping terms in the Hamiltonian have the form

$$H_w = \frac{R_1}{2} (k_+^3 + k_-^3) \mathbb{I} \otimes \sigma_y + i \frac{R_2}{2} (k_+^3 - k_-^3) \sigma_z \otimes \sigma_x, \quad (12)$$

where R_1 and R_2 are material-specific parameters. These terms were ignored because they increase the complexity of the dispersion and eigenstates. However, we did do some calculations with them to approximate their effect on the proper spin current. We find that the warping terms have no effect on the magnitude of the spin current at lower Fermi energies where our model is valid.

V. DISCUSSION

Here we have demonstrated a straightforward method for calculating the proper spin current due to impurity scattering. This, along with our previous work on intrinsic spin currents [44], provides straightforward formulas for calculating the total proper spin current. This method can be applied generally to other systems of interest, and it can be applied to any system, for example van der Waals heterostructures and other exotic materials [23–33]. In this work, we applied our method for calculating the proper spin current to topological insulators and calculated the spin conductivity of Bi_2Se_3 , Bi_2Te_3 and Sb_2Te_3 both with and without hexagonal warping. We find that the “side jump” scattering term \hat{J}_E is the dominant contribution to the extrinsic spin Hall effect. Furthermore, we find that the extrinsic spin-Hall effect is of a similar magnitude to the intrinsic Hall effect in topological insulators [44]; this is demonstrated in Fig. 2, where both extrinsic and intrinsic spin conductivities are plotted. We find that when the Fermi

energy is in the conduction band, the spin conductivity of the bulk TI states is $\sigma_{zx}^y \sim 10^3 (\hbar/2e) \Omega^{-1} \text{m}^{-1}$.

In the present study, we focused solely on short-ranged scalar impurities. However, our methodology allows for the inclusion of more complex scattering potentials, and it can be applied to further investigations of the spin-Hall effect, incorporating spin-orbit scattering beyond what we have considered. Our spin current equations are applicable to both 3D and 2D systems. In the case of 2D systems, additional consideration may be required for weak localization effects, which can be incorporated through modifications to the linear-response formalism outlined here [125].

A. Approaches to the evaluation of the proper spin current

Following the proposal of the proper spin current [60], various approaches have been devised to tackle the highly nontrivial task of its evaluation. The approaches adopted include the quantum-mechanical methodology of this work and Ref. [44], the semiclassical method of Ref. [45], and the Keldysh method of Ref. [68]. Two features shared by all transport theories relevant to this study, including the Kubo formula, are the treatment of the external potential as a classical quantity $V(\mathbf{r})$, and the assumption $(\varepsilon_F \tau / \hbar) \gg 1$, which ensures that quantum interference effects are suppressed. Beyond this point, there are important differences between the approaches mentioned above, and unfortunately a direct comparison is not straightforward for the reasons outlined below.

The quantum kinetic theory presented in this work, which complements the intrinsic results of Ref. [44], treats the response of the electronic system fully quantum mechanically and is equivalent to the Kubo linear-response formalism (the *family tree* of linear-response theories has been outlined in Ref. [78]). The aim of the calculation is to determine the expectation value of the operator $d/dt(\hat{r}\hat{s})$, which is decomposed into the conventional spin current and the torque dipole. Whereas a special technique is developed to treat the position operator appearing in the torque dipole, the methodology follows the standard philosophy of nonequilibrium quantum mechanics.

The approach of Ref. [45] is based on semiclassical wavepacket dynamics, which require one to treat the position and momentum of an electron simultaneously within a framework consistent with the uncertainty principle. The formalism constructs the spin current by adding a number of distinct contributions following the prescriptions of classical physics and Maxwell's equations, and referencing the center of mass of a wave packet.

Finally, Ref. [68] employed the Keldysh approach while at the same time considering fictitious electric and magnetic fields that are nonuniform in the center-of-mass coordinates. In the sense that this approach mixes position and momentum space, it also involves a semiclassical approximation, contained in a gradient expansion, although at the end the nonuniformity is removed by taking the limit of the center-of-mass coordinate approaching zero.

The various terms obtained in Refs. [44,45] cannot be matched one by one, and a direct comparison of our work with Ref. [45] requires further analysis. The presence of the torque dipole is justified by the arguments presented in Ref. [60],

where this quantity was shown to aid in the formulation of a conserved spin current. The arguments of Ref. [60] can also be recast in fully quantum-mechanical language by employing the Wigner transformation. The main finding of this work was that, taking the conventional spin current \hat{s} , \hat{v} and adding the torque dipole \hat{r} , $d\hat{s}/dt$, one arrives at the new definition $d/dt(\hat{r}\hat{s})$, which is conserved in many circumstances. In this context, no such general argument can be found for the torque quadrupole, and we conclude that the torque quadrupole appears in Ref. [45] due to considerations specific to the semiclassical method employed there. In other words, one cannot simply define a quantum-mechanical torque quadrupole operator and add it on to the method of Ref. [44] and the present manuscript—such a procedure cannot be justified on macroscopic grounds. One important difference is that the torque quadrupole appears in the derivation in Ref. [45], since Ref. [45] considers nonuniform systems to first order in the spatial gradient, whereas we only consider uniform systems. Although not attempted here, our approach can be applied to nonuniform systems through use of a Wigner transform along the lines of Ref. [116].

Nevertheless, we wish to stress that, apart from the position of the spin matrix elements, all the fundamental features of our results are shared by those of Ref. [45]: spin transport is Hall transport, the response function is expressed in terms of diagonal spin matrix elements and topological quantities, and the conditions for the spin current to be nonzero in these two approaches are essentially identical.

In contrast, the evaluation of the proper spin current following the method of Ref. [68] results in a spin current that vanishes in spin-1/2 systems regardless of the model. This is at variance with our findings and those of Ref. [45]. A detailed comparison is hampered at this stage by the fact that our theory does not rely on fictitious electromagnetic fields or on an explicit gradient expansion, and by the lack of generic formulas in Ref. [68], whose results were focused primarily on specific models.

B. The spin-Hall effect in topological insulators

We employed an effective 2×2 spin-orbit Hamiltonian used in Ref. [116] for our analysis. We find that the spin currents linear in the scattering time— \mathcal{J}_{zx}^x , where $\mathbf{m} \parallel \hat{z}$, and \mathcal{J}_{zx}^z , where $\mathbf{m} \parallel \hat{x}$ —have identical magnitude. This is the case in both our analysis and in the numerical calculation. Conversely, the spin currents independent of disorder strength are of different orders in the spin-orbit field for different orientations of the Zeeman field. This implies that at low Fermi energies, $E_F < 10$ meV, there will be large differences in the magnitude of the spin current \mathcal{J}_{zx}^y . From our analysis, we expect $|\mathcal{J}_{zx,m_y}^y| \gg |\mathcal{J}_{zx,m_x}^y| \gg |\mathcal{J}_{zx,m_z}^y|$ and that \mathcal{J}_{zx,m_x}^y will have the opposite sign to \mathcal{J}_{zx,m_x}^y and \mathcal{J}_{zx,m_z}^y . This is consistent with our numerical results at low Fermi energies as shown in Fig. 5, where the extrinsic spin conductivity σ_{zx}^y has been plotted for three different Zeeman field directions. Furthermore, we find that even at larger Fermi energies beyond where the effective Hamiltonian is valid, this hierarchy in spin current magnitudes for each Zeeman field orientation still exists. For Zeeman fields oriented $\parallel \hat{z}$ or \hat{x} , the intrinsic and extrinsic spin conductivities σ_{zx}^y have opposite signs and the magnitude of the

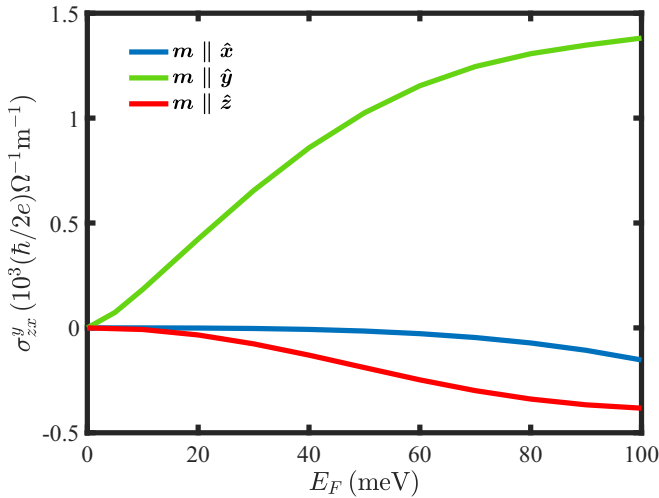


FIG. 5. The extrinsic spin-Hall conductivity σ_{zx}^y vs the Fermi energy E_F for the TI bulk states with different Zeeman field orientations. For Bi_2Se_3 with Zeeman energy $|m| = 10 \mu\text{eV}$ (Bi_2Se_3 parameters from Ref. [77]).

intrinsic spin conductivity increases slower than the extrinsic spin conductivity while increasing the Fermi energy. Hence, for these cases the spin conductivity will be at a maximum when the Fermi energy is in the band gap, though this may not be the case for larger Fermi energies beyond where our model is accurate. Conversely, for a Zeeman field $\parallel \hat{y}$ the extrinsic and intrinsic spin conductivities will have the same sign and add constructively. This is demonstrated in Fig. 6, in which we have plotted the total spin conductivity σ_{zx}^y including both intrinsic and extrinsic contributions.

It should be noted that the dependence of the spin current on the direction of the spin-orbit field is a smoking gun for the measurement of the extrinsic spin-Hall effect. This can be tested using a TI/FM sample by varying the orientation of

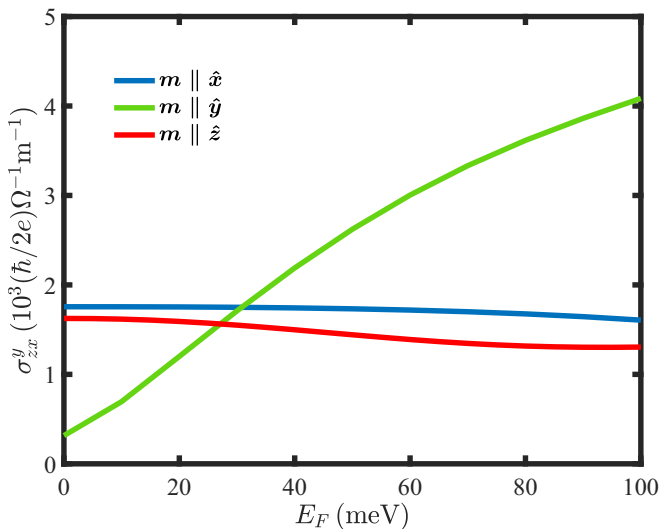


FIG. 6. The total spin-Hall conductivity σ_{zx}^y (intrinsic and extrinsic) vs the Fermi energy E_F for the TI bulk states in Bi_2Se_3 with Zeeman energy $|m| = 10 \mu\text{eV}$ (Bi_2Se_3 parameters from Ref. [77]).

a small external magnetic field and measuring the changes in the size of the spin torque. Although the orbital effects of a magnetic field are not considered in this work, as long as the magnetic field is small enough any orbital effects should be negligible. The dependence of the spin-Hall effect on the Zeeman field and the spin-orbit field Ω has interesting parallels to the previous work on the bulk spin transfer torque [116].

The results we have presented for TIs have in-plane x - y symmetry. For example, our results with $m \parallel \hat{z}$ are the same for the electric fields oriented $\parallel \hat{x}$ and $\parallel \hat{y}$, and we find that $\sigma_{zx}^x = \sigma_{zy}^y$ and $\sigma_{zx}^y = -\sigma_{zy}^x$. This holds even when including the hexagonal warping terms due to their threefold rotational symmetry. The spin conductivities will differ for an out-of-plane electric field, but we have not studied such a configuration here as it is not often used in spin torque devices.

C. Spin torques in topological insulators

Spin torques in topological insulator spin torque devices are known to be driven by various mechanisms, including the spin-Hall effect in the bulk [43,126,127], the Rashba-Edelstein effect (REE) in the surface states, and the spin transfer torque (STT) due to the proximity effect with the adjacent magnetic layer [116,128]. In the field of TI spin torques, a crucial yet unresolved question pertains to determining the relative magnitude of each spin torque mechanism. The Rashba-Edelstein effect is known to be sizable at the surface topological insulators [126,129–132]. However, it has been shown that the chemical potential lies in the bulk TI conduction band for most TI/FM devices [133,134], and that bulk transport dominates in a certain parameter regime [121]. So, spin torques due to the bulk states are unable to be neglected. Furthermore, recently the spin density due to the STT mechanism in the bulk states was shown potentially to be of the same order of magnitude as the spin density generated by the REE in the surface states [116]. Given the low conductivity of TI samples, it can be inferred that samples are generally quite dirty. Hence, it is also important to consider extrinsic effects in these materials. We find our calculated spin conductivities to be roughly one to two orders of magnitude smaller than those recorded in experiment, $\sigma_s = (0.15-2) \times 10^5 (\hbar/2e) \Omega^{-1} \text{m}^{-1}$ [95,111,112,114]. This indicates that the large charge to spin conversion efficiency of TIs measured in experiment is largely due to other spin torque mechanisms and not the spin-Hall effect. Although experimental works calculate the spin conductivity, which is related to the spin-Hall effect, what is measured is the spin torque, which has contributions from spin polarizations generated via other mechanisms [135].

It must be noted that directly relating the spin current to a spin torque is difficult, due to the complexity of accurately calculating the effect of the TI/FM interface on the spin current. Although in our analysis and in most common experimental analysis the spin current is treated as directly proportional to the torque, this is generally incorrect. Our calculations are of spin currents in the bulk of the TI, and hence they do not directly relate to the spin conductivity measured in experiment. However, despite this we are still confident in our claim that the bulk SHE will contribute negligibly to the spin torque, as we expect these interface effects to decohere

and reduce the magnitude of the spin current coming from the bulk. Spin memory loss [136,137] can occur at the interface, which would reduce the effect of the bulk spin-Hall effect on the spin torque, supporting the view proposed here that the SHE is negligible in topological insulator spin torques. Furthermore, a previous study employing the conventional spin current Kubo formula [138] showed that inhomogeneous spin-orbit coupling at the interface due to roughness may also generate a spin current [139,140].

Our calculations show that the extrinsic spin-Hall effect will generate both damping and fieldlike spin currents. We determine that the spin currents are to be fieldlike or dampinglike based on their symmetry. Furthermore, we predict these spin currents can be of a similar magnitude. However, they exhibit specific differences, for example the fieldlike current is independent of impurity density whereas the dampinglike current is dependent on the impurity density. The dampinglike current is linear in the scattering time and hence should be larger in cleaner samples. The fieldlike current has no such dependence, furthermore the intrinsic spin conductivity is also purely fieldlike. Hence, neglecting interface effects, the fieldlike contribution to the spin torque due to the spin Hall effect will be entirely independent of the impurity density. Although we predict the dampinglike spin current to likely be small, due to its dependence on the impurity density it has the possibility to be of a comparable size to the fieldlike current in very clean samples with high charge conductivity. Hence, if the spin-Hall effect is a significant part of the TI spin torque, we may expect the spin conductivity to be significantly smaller in more disordered samples. However, a study of spin torques in sputtered topological insulators measured an exceedingly large spin conductivity of $\sigma_s = 1.5 \times 10^5 (\hbar/2e) \Omega^{-1} \text{m}^{-1}$ [114]. This further indicates that the spin-Hall effect is likely negligible in TI spin torques.

The results in this paper combined with the results in Refs. [44,116] give a comprehensive analysis of spin torques

stemming from the TI bulk states. The bulk states give two contributions to the spin torque, namely spin currents from the spin-Hall effect and spin polarizations due to the spin transfer torque mechanism. The spin-Hall effect calculated is small and contributes negligibly to the total spin torque. The bulk spin transfer torque calculated with an idealized model is negligible when compared to the surface state torque, but it can potentially be large in real samples. So, the only bulk TI spin torque contribution that can compete with the Rashba-Edelstein effect in the surface states is the spin transfer torque. This is consistent with experimental results that find the spin torque efficiency increases for thinner TI samples [111], which implies that states at or near the interface are the dominant contribution to the spin torque and that purely bulk contributions are negligible. These results do not preclude the possibility of a substantial spin transfer torque, since spin polarizations from this effect are localized near the interface where there is a proximity-induced magnetization in the topological insulator.

VI. CONCLUSION

In conclusion, we formulated a fully quantum-mechanical way of calculating the extrinsic spin-Hall effect. We applied it to topological insulator systems to investigate the role of the extrinsic spin-Hall effect in topological insulator spin torques. We found the extrinsic spin conductivity to be roughly two orders of magnitude smaller than those reported in experiment, and we concluded that its role in spin torques is negligible.

ACKNOWLEDGMENTS

This project was supported by the Australian Research Council Future Fellowship FT190100062. J.H.C. acknowledges support from an Australian Government Research Training Program (RTP) Scholarship.

-
- [1] B. K. Nikolic, K. Dolui, M. D. Petrovic, P. Plechac, T. Markussen, and K. Stokbro, *First-Principles Quantum Transport Modeling of Spin-Transfer and Spin-Orbit Torques in Magnetic Multilayers* (Springer, Cham, 2018).
 - [2] A. Manchon, J. Železný, I. M. Miron, T. Jungwirth, J. Sinova, A. Thiaville, K. Garello, and P. Gambardella, Current-induced spin-orbit torques in ferromagnetic and antiferromagnetic systems, *Rev. Mod. Phys.* **91**, 035004 (2019).
 - [3] A. Brataas, A. D. Kent, and H. Ohno, Current-induced torques in magnetic materials, *Nat. Mater.* **11**, 372 (2012).
 - [4] H. Wu, A. Chen, P. Zhang, H. He, J. Nance, C. Guo, J. Sasaki, T. Shirokura, P. N. Hai, B. Fang *et al.*, Magnetic memory driven by topological insulators, *Nat. Commun.* **12**, 6251 (2021).
 - [5] Q. Shao, P. Li, L. Liu, H. Yang, S. Fukami, A. Razavi, H. Wu, K. Wang, F. Freimuth, Y. Mokrousov, M. D. Stiles, S. Emori, A. Hoffmann, J. Akerman, K. Roy, J.-P. Wang, S.-H. Yang, K. Garello, and W. Zhang, Roadmap of spin-orbit torques, *IEEE Trans. Magn.* **57**, 1 (2021).
 - [6] R. Ramaswamy, J. M. Lee, K. Cai, and H. Yang, Recent advances in spin-orbit torques: Moving towards device applications, *Appl. Phys. Rev.* **5**, 031107 (2018).
 - [7] M. I. Dyakonov and V. I. Perel, Possibility of orienting electron spins with current, *JETP Lett. USSR* **13**, 467 (1971).
 - [8] M. Dyakonov and V. Perel, Current-induced spin orientation of electrons in semiconductors, *Phys. Lett. A* **35**, 459 (1971).
 - [9] J. E. Hirsch, Spin Hall effect, *Phys. Rev. Lett.* **83**, 1834 (1999).
 - [10] S. Murakami, N. Nagaosa, and S.-C. Zhang, Dissipationless quantum spin current at room temperature, *Science* **301**, 1348 (2003).
 - [11] J. Sinova, D. Culcer, Q. Niu, N. A. Sinitsyn, T. Jungwirth, and A. H. MacDonald, Universal intrinsic spin Hall effect, *Phys. Rev. Lett.* **92**, 126603 (2004).
 - [12] J. Wunderlich, B. Kaestner, J. Sinova, and T. Jungwirth, Experimental observation of the spin-Hall effect in a two-dimensional spin-orbit coupled semiconductor system, *Phys. Rev. Lett.* **94**, 047204 (2005).

- [13] Y. K. Kato, R. C. Myers, A. C. Gossard, and D. D. Awschalom, Observation of the spin Hall effect in semiconductors, *Science* **306**, 1910 (2004).
- [14] J. Fan and J. Eom, Direct electrical observation of spin Hall effect in Bi film, *Appl. Phys. Lett.* **92**, 142101 (2008).
- [15] Y. Niimi, M. Morota, D. H. Wei, C. Deranlot, M. Basletic, A. Hamzic, A. Fert, and Y. Otani, Extrinsic spin Hall effect induced by iridium impurities in copper, *Phys. Rev. Lett.* **106**, 126601 (2011).
- [16] M. Morota, Y. Niimi, K. Ohnishi, D. H. Wei, T. Tanaka, H. Kontani, T. Kimura, and Y. Otani, Indication of intrinsic spin Hall effect in $4d$ and $5d$ transition metals, *Phys. Rev. B* **83**, 174405 (2011).
- [17] L. Liu, C.-F. Pai, Y. Li, H. W. Tseng, D. C. Ralph, and R. A. Buhrman, Spin-torque switching with the giant spin Hall effect of tantalum, *Science* **336**, 555 (2012).
- [18] C.-F. Pai, L. Liu, Y. Li, H. W. Tseng, D. C. Ralph, and R. A. Buhrman, Spin transfer torque devices utilizing the giant spin Hall effect of tungsten, *Appl. Phys. Lett.* **101**, 122404 (2012).
- [19] Y. Niimi, Y. Kawanishi, D. H. Wei, C. Deranlot, H. X. Yang, M. Chshiev, T. Valet, A. Fert, and Y. Otani, Giant spin Hall effect induced by skew scattering from bismuth impurities inside thin film CuBi alloys, *Phys. Rev. Lett.* **109**, 156602 (2012).
- [20] G. Mihajlović, J. E. Pearson, M. A. Garcia, S. D. Bader, and A. Hoffmann, Negative nonlocal resistance in mesoscopic gold Hall bars: Absence of the giant spin Hall effect, *Phys. Rev. Lett.* **103**, 166601 (2009).
- [21] O. M. J. van 't Erve, A. T. Hanbicki, K. M. McCreary, C. H. Li, and B. T. Jonker, Optical detection of spin Hall effect in metals, *Appl. Phys. Lett.* **104**, 172402 (2014).
- [22] R. Chu, L. Liu, B. Cui, W. Liu, T. An, X. Ren, T. Miao, B. Cheng, and J. Hu, Electrical control of spin Hall effect in Pt by hydrogen ion adsorption and desorption, *ACS Nano* **16**, 16077 (2022).
- [23] P. Wang, A. Migliorini, S.-H. Yang, J.-C. Jeon, I. Kostanovskiy, H. Meyerheim, H. Han, H. Deniz, and S. S. P. Parkin, Giant spin Hall effect and spin-orbit torques in $5d$ transition metal-aluminum alloys from extrinsic scattering, *Adv. Mater.* **34**, 2109406 (2022).
- [24] P. K. Muduli, T. Higo, T. Nishikawa, D. Qu, H. Isshiki, K. Kondou, D. Nishio-Hamane, S. Nakatsuji, and Y. C. Otani, Evaluation of spin diffusion length and spin Hall angle of the antiferromagnetic Weyl semimetal Mn_3Sn , *Phys. Rev. B* **99**, 184425 (2019).
- [25] B. Zhao, D. Khokhriakov, Y. Zhang, H. Fu, B. Karpiak, A. M. Hoque, X. Xu, Y. Jiang, B. Yan, and S. P. Dash, Observation of charge to spin conversion in Weyl semimetal WTe_2 at room temperature, *Phys. Rev. Res.* **2**, 013286 (2020).
- [26] A. Avsar, J. Y. Tan, T. Taychatanapat, J. Balakrishnan, G. Koon, Y. Yeo, J. Lahiri, A. Carvalho, A. Rodin, E. O'Farrell *et al.*, Spin-orbit proximity effect in graphene, *Nat. Commun.* **5**, 4875 (2014).
- [27] L. A. Benítez, W. Savero Torres, J. F. Sierra, M. Timmermans, J. H. Garcia, S. Roche, M. V. Costache, and S. O. Valenzuela, Tunable room-temperature spin galvanic and spin Hall effects in van der Waals heterostructures, *Nat. Mater.* **19**, 170 (2020).
- [28] C. Safeer, J. Ingla-Aynés, F. Herling, J. H. Garcia, M. Vila, N. Ontoso, M. R. Calvo, S. Roche, L. E. Hueso, and F. Casanova, Room-temperature spin Hall effect in graphene/MoS₂ van der Waals heterostructures, *Nano Lett.* **19**, 1074 (2019).
- [29] C. Safeer, J. Ingla-Aynés, N. Ontoso, F. Herling, W. Yan, L. E. Hueso, and F. Casanova, Spin Hall effect in bilayer graphene combined with an insulator up to room temperature, *Nano Lett.* **20**, 4573 (2020).
- [30] G. Dastgeer, A. M. Afzal, S. H. A. Jaffery, M. Imran, M. A. Assiri, and S. Nisar, Gate modulation of the spin current in graphene/WSe₂ van der Waals heterostructure at room temperature, *J. Alloys Compd.* **919**, 165815 (2022).
- [31] F. Herling, C. Safeer, J. Ingla-Aynés, N. Ontoso, L. E. Hueso, and F. Casanova, Gate tunability of highly efficient spin-to-charge conversion by spin Hall effect in graphene proximitized with WSe₂, *APL Mater.* **8**, 071103 (2020).
- [32] T. S. Ghiasi, A. A. Kaverzin, P. J. Blah, and B. J. Van Wees, Charge-to-spin conversion by the Rashba-Edelstein effect in two-dimensional van der Waals heterostructures up to room temperature, *Nano Lett.* **19**, 5959 (2019).
- [33] A. M. Hoque, B. Zhao, D. Khokhriakov, P. Muduli, and S. P. Dash, Charge to spin conversion in van der Waals metal NbSe₂, *Appl. Phys. Lett.* **121**, 242404 (2022).
- [34] E. Saitoh, M. Ueda, H. Miyajima, and G. Tatara, Conversion of spin current into charge current at room temperature: Inverse spin-Hall effect, *Appl. Phys. Lett.* **88**, 182509 (2006).
- [35] K. Ando, S. Takahashi, J. Ieda, Y. Kajiwara, H. Nakayama, T. Yoshino, K. Harii, Y. Fujikawa, M. Matsuo, S. Maekawa *et al.*, Inverse spin-Hall effect induced by spin pumping in metallic system, *J. Appl. Phys.* **109**, 103913 (2011).
- [36] S. O. Valenzuela and M. Tinkham, Direct electronic measurement of the spin Hall effect, *Nature (London)* **442**, 176 (2006).
- [37] M. Kimata, H. Chen, K. Kondou, S. Sugimoto, P. K. Muduli, M. Ikhlas, Y. Otori, T. Tomita, A. H. MacDonald, S. Nakatsuji *et al.*, Magnetic and magnetic inverse spin Hall effects in a non-collinear antiferromagnet, *Nature (London)* **565**, 627 (2019).
- [38] Z. Zhu, X. Zheng, G. Li, H. Bai, J. Su, Y. Zhang, and J.-W. Cai, Strong spin orientation-dependent spin current diffusion and inverse spin Hall effect in a ferromagnetic metal, *NPG Asia Mater.* **12**, 12 (2020).
- [39] L. Huang, Y. Zhou, H. Qiu, H. Bai, C. Chen, W. Yu, L. Liao, T. Guo, F. Pan, B. Jin *et al.*, Antiferromagnetic inverse spin Hall effect, *Adv. Mater.* **34**, 2205988 (2022).
- [40] A. Yagmur, S. Sumi, H. Awano, and K. Tanabe, Magnetization-dependent inverse spin Hall effect in compensated ferrimagnet TbCo alloys, *Phys. Rev. B* **103**, 214408 (2021).
- [41] B. B. Singh, K. Roy, J. A. Chelvane, and S. Bedanta, Inverse spin Hall effect and spin pumping in the polycrystalline non-collinear antiferromagnetic Mn_3Ga , *Phys. Rev. B* **102**, 174444 (2020).
- [42] R. S. Akzyanov and A. L. Rakhmanov, Bulk and surface spin conductivity in topological insulators with hexagonal warping, *Phys. Rev. B* **99**, 045436 (2019).
- [43] S. Ghosh and A. Manchon, Spin-orbit torque in a three-dimensional topological insulator-ferromagnet heterostructure: Crossover between bulk and surface transport, *Phys. Rev. B* **97**, 134402 (2018).
- [44] H. Liu, J. H. Cullen, and D. Culcer, Topological nature of the proper spin current and the spin-Hall torque, *Phys. Rev. B* **108**, 195434 (2023).

- [45] C. Xiao and Q. Niu, Conserved current of nonconserved quantities, *Phys. Rev. B* **104**, L241411 (2021).
- [46] D. Schmeltzer, Topological spin current induced by noncommuting coordinates: An application to the spin-Hall effect, *Phys. Rev. B* **73**, 165301 (2006).
- [47] A. Zhang and J.-W. Rhim, Geometric origin of intrinsic spin Hall effect in an inhomogeneous electric field, *Commun. Phys.* **5**, 195 (2022).
- [48] M.-F. Yang and M.-C. Chang, Středa-like formula in the spin Hall effect, *Phys. Rev. B* **73**, 073304 (2006).
- [49] H. Zhang, Z. Ma, and J.-F. Liu, Equilibrium spin current in graphene with Rashba spin-orbit coupling, *Sci. Rep.* **4**, 6464 (2014).
- [50] F. Matusalem, M. Marques, L. K. Teles, L. Matthes, J. Furthmüller, and F. Bechstedt, Quantization of spin Hall conductivity in two-dimensional topological insulators versus symmetry and spin-orbit interaction, *Phys. Rev. B* **100**, 245430 (2019).
- [51] L. Ulčakar, J. Mravlje, A. Ramšak, and T. Rejec, Slow quenches in two-dimensional time-reversal symmetric z_2 topological insulators, *Phys. Rev. B* **97**, 195127 (2018).
- [52] C. Şahin and M. E. Flatté, Tunable giant spin Hall conductivities in a strong spin-orbit semimetal: $\text{Bi}_{1-x}\text{Sb}_x$, *Phys. Rev. Lett.* **114**, 107201 (2015).
- [53] Y. Sun, Y. Zhang, C. Felser, and B. Yan, Strong intrinsic spin Hall effect in the taas family of Weyl semimetals, *Phys. Rev. Lett.* **117**, 146403 (2016).
- [54] O. V. Dimitrova, Spin-Hall conductivity in a two-dimensional Rashba electron gas, *Phys. Rev. B* **71**, 245327 (2005).
- [55] P.-Q. Jin and Y.-Q. Li, Generalized Kubo formula for spin transport: A theory of linear response to non-abelian fields, *Phys. Rev. B* **74**, 085315 (2006).
- [56] G. Tatara, Spin correlation function theory of spin-charge conversion effects, *Phys. Rev. B* **98**, 174422 (2018).
- [57] A. Shitade and G. Tatara, Spin accumulation without spin current, *Phys. Rev. B* **105**, L201202 (2022).
- [58] Y. Gao, D. Vanderbilt, and D. Xiao, Microscopic theory of spin toroidization in periodic crystals, *Phys. Rev. B* **97**, 134423 (2018).
- [59] A. Shitade, A. Daido, and Y. Yanase, Theory of spin magnetic quadrupole moment and temperature-gradient-induced magnetization, *Phys. Rev. B* **99**, 024404 (2019).
- [60] D. Culcer, J. Sinova, N. A. Sinitsyn, T. Jungwirth, A. H. MacDonald, and Q. Niu, Semiclassical spin transport in spin-orbit-coupled bands, *Phys. Rev. Lett.* **93**, 046602 (2004).
- [61] S. Murakami, N. Nagaosa, and S.-C. Zhang, $\text{SU}(2)$ non-abelian holonomy and dissipationless spin current in semiconductors, *Phys. Rev. B* **69**, 235206 (2004).
- [62] F. Freimuth, S. Blügel, and Y. Mokrousov, Anisotropic spin Hall effect from first principles, *Phys. Rev. Lett.* **105**, 246602 (2010).
- [63] C. Gorini, R. Raimondi, and P. Schwab, Onsager relations in a two-dimensional electron gas with spin-orbit coupling, *Phys. Rev. Lett.* **109**, 246604 (2012).
- [64] C. Xiao, J. Zhu, B. Xiong, and Q. Niu, Conserved spin current for the mott relation, *Phys. Rev. B* **98**, 081401(R) (2018).
- [65] J. Shi, P. Zhang, D. Xiao, and Q. Niu, Proper definition of spin current in spin-orbit coupled systems, *Phys. Rev. Lett.* **96**, 076604 (2006).
- [66] P. Zhang, Z. Wang, J. Shi, D. Xiao, and Q. Niu, Theory of conserved spin current and its application to a two-dimensional hole gas, *Phys. Rev. B* **77**, 075304 (2008).
- [67] D. Monaco and L. Ulčakar, Spin Hall conductivity in insulators with nonconserved spin, *Phys. Rev. B* **102**, 125138 (2020).
- [68] N. Sugimoto, S. Onoda, S. Murakami, and N. Nagaosa, Spin Hall effect of a conserved current: Conditions for a nonzero spin Hall current, *Phys. Rev. B* **73**, 113305 (2006).
- [69] E. M. Hankiewicz, G. Vignale, and M. E. Flatté, Spin-Hall effect in a [110] GaAs quantum well, *Phys. Rev. Lett.* **97**, 266601 (2006).
- [70] J. I. Inoue, G. E. W. Bauer, and L. W. Molenkamp, Suppression of the persistent spin Hall current by defect scattering, *Phys. Rev. B* **70**, 041303(R) (2004).
- [71] R. Raimondi and P. Schwab, Spin-Hall effect in a disordered two-dimensional electron system, *Phys. Rev. B* **71**, 033311 (2005).
- [72] E. G. Mishchenko, A. V. Shytov, and B. I. Halperin, Spin current and polarization in impure two-dimensional electron systems with spin-orbit coupling, *Phys. Rev. Lett.* **93**, 226602 (2004).
- [73] S. Y. Liu, X. L. Lei, and N. J. M. Horing, Vanishing spin-Hall current in a diffusive Rashba two-dimensional electron system: A quantum boltzmann equation approach, *Phys. Rev. B* **73**, 035323 (2006).
- [74] N. A. Sinitsyn, A. H. MacDonald, T. Jungwirth, V. K. Dugaev, and J. Sinova, Anomalous Hall effect in a two-dimensional Dirac band: The link between the Kubo-Středa formula and the semiclassical boltzmann equation approach, *Phys. Rev. B* **75**, 045315 (2007).
- [75] N. Sinitsyn, Semiclassical theories of the anomalous Hall effect, *J. Phys.: Condens. Matter* **20**, 023201 (2008).
- [76] N. Nagaosa, J. Sinova, S. Onoda, A. H. MacDonald, and N. P. Ong, Anomalous Hall effect, *Rev. Mod. Phys.* **82**, 1539 (2010).
- [77] C.-X. Liu, X.-L. Qi, H. J. Zhang, X. Dai, Z. Fang, and S.-C. Zhang, Model hamiltonian for topological insulators, *Phys. Rev. B* **82**, 045122 (2010).
- [78] R. B. Atencia, Q. Niu, and D. Culcer, Semiclassical response of disordered conductors: Extrinsic carrier velocity and spin and field-corrected collision integral, *Phys. Rev. Res.* **4**, 013001 (2022).
- [79] D. Culcer, E. M. Hankiewicz, G. Vignale, and R. Winkler, Side jumps in the spin Hall effect: Construction of the boltzmann collision integral, *Phys. Rev. B* **81**, 125332 (2010).
- [80] D. Culcer, E. H. Hwang, T. D. Stanescu, and S. DasSarma, Two-dimensional surface charge transport in topological insulators, *Phys. Rev. B* **82**, 155457 (2010).
- [81] X. Bi, P. He, E. M. Hankiewicz, R. Winkler, G. Vignale, and D. Culcer, Anomalous spin precession and spin Hall effect in semiconductor quantum wells, *Phys. Rev. B* **88**, 035316 (2013).
- [82] Q. Lu, P. Li, Z. Guo, G. Dong, B. Peng, X. Zha, T. Min, Z. Zhou, and M. Liu, Giant tunable spin Hall angle in sputtered Bi_2Se_3 controlled by an electric field, *Nat. Commun.* **13**, 1650 (2022).
- [83] M. Mogi, K. Yasuda, R. Fujimura, R. Yoshimi, N. Ogawa, A. Tsukazaki, M. Kawamura, K. S. Takahashi, M. Kawasaki, and Y. Tokura, Current-induced switching of proximity-

- induced ferromagnetic surface states in a topological insulator, *Nat. Commun.* **12**, 1404 (2021).
- [84] X. Che, Q. Pan, B. Vareskic, J. Zou, L. Pan, P. Zhang, G. Yin, H. Wu, Q. Shao, P. Deng *et al.*, Strongly surface state carrier-dependent spin-orbit torque in magnetic topological insulators, *Adv. Mater.* **32**, 1907661 (2020).
- [85] P. Li, J. Kally, S. S.-L. Zhang, T. Pillsbury, J. Ding, G. Csaba, J. Ding, J. S. Jiang, Y. Liu, R. Sinclair, C. Bi, A. DeMann, G. Rimal, W. Zhang, S. B. Field, J. Tang, W. Wang, O. G. Heinonen, V. Novosad, A. Hoffmann *et al.*, Magnetization switching using topological surface states, *Sci. Adv.* **5**, eaaw3415 (2019).
- [86] C. H. Li, O. M. J. Van 't Erve, J. T. Robinson, Y. Liu, L. Li, and B. T. Jonker, Electrical detection of charge-current-induced spin polarization due to spin-momentum locking in Bi_2Se_3 , *Nat. Nanotechnol.* **9**, 218 (2014).
- [87] Y. Liu, J. Besbas, Y. Wang, P. He, M. Chen, D. Zhu, Y. Wu, J. M. Lee, L. Wang, J. Moon *et al.*, Direct visualization of current-induced spin accumulation in topological insulators, *Nat. Commun.* **9**, 2492 (2018).
- [88] Q. Zhang, K. S. Chan, and J. Li, Spin-transfer torque generated in graphene based topological insulator heterostructures, *Sci. Rep.* **8**, 4343 (2018).
- [89] M. Rodriguez-Vega, G. Schwiete, J. Sinova, and E. Rossi, Giant Edelstein effect in topological-insulator-graphene heterostructures, *Phys. Rev. B* **96**, 235419 (2017).
- [90] K. Song, D. Soriano, A. W. Cummings, R. Robles, P. Ordejón, and S. Roche, Spin proximity effects in graphene/topological insulator heterostructures, *Nano Lett.* **18**, 2033 (2018).
- [91] S. Shi, A. Wang, Y. Wang, R. Ramaswamy, L. Shen, J. Moon, D. Zhu, J. Yu, S. Oh, Y. Feng *et al.*, Efficient charge-spin conversion and magnetization switching through the Rashba effect at topological-insulator/ag interfaces, *Phys. Rev. B* **97**, 041115(R) (2018).
- [92] F. Bonell, M. Goto, G. Sauthier, J. F. Sierra, A. I. Figueroa, M. V. Costache, S. Miwa, Y. Suzuki, and S. O. Valenzuela, Control of spin-orbit torques by interface engineering in topological insulator heterostructures, *Nano Lett.* **20**, 5893 (2020).
- [93] H. Wu, P. Zhang, P. Deng, Q. Lan, Q. Pan, S. A. Razavi, X. Che, L. Huang, B. Dai, K. Wong *et al.*, Room-temperature spin-orbit torque from topological surface states, *Phys. Rev. Lett.* **123**, 207205 (2019).
- [94] X. Liu, D. Wu, L. Liao, P. Chen, Y. Zhang, F. Xue, Q. Yao, C. Song, K. L. Wang, and X. Kou, Temperature dependence of spin-orbit torque-driven magnetization switching in in situ grown $\text{Bi}_2\text{Te}_3/\text{MnTe}$ heterostructures, *Appl. Phys. Lett.* **118**, 112406 (2021).
- [95] A. R. Mellnik, J. S. Lee, A. Richardella, J. L. Grab, P. J. Mintun, M. H. Fischer, A. Vaezi, A. Manchon, E.-A. Kim, N. Samarth, and D. C. Ralph, Spin-transfer torque generated by a topological insulator, *Nature (London)* **511**, 449 (2014).
- [96] Y. Wang, P. Deorani, K. Banerjee, N. Koirala, M. Brahlek, S. Oh, and H. Yang, Topological surface states originated spin-orbit torques in Bi_2Se_3 , *Phys. Rev. Lett.* **114**, 257202 (2015).
- [97] M. Jamali, J. S. Lee, J. S. Jeong, F. Mahfouzi, Y. Lv, Z. Zhao, B. K. Nikolić, K. A. Mkhoyan, N. Samarth, and J.-P. Wang, Giant spin pumping and inverse spin Hall effect in the presence of surface and bulk spin-orbit coupling of topological insulator Bi_2Se_3 , *Nano Lett.* **15**, 7126 (2015).
- [98] K. Kondou, R. Yoshimi, A. Tsukazaki, Y. Fukuma, J. Matsuno, K. S. Takahashi, M. Kawasaki, Y. Tokura, and Y. Otani, Fermi-level-dependent charge-to-spin current conversion by Dirac surface states of topological insulators, *Nat. Phys.* **12**, 1027 (2016).
- [99] Y. T. Fanchiang, K. H. M. Chen, C. C. Tseng, C. C. Chen, C. K. Cheng, S. R. Yang, C. N. Wu, S. F. Lee, M. Hong, and J. Kwo, Strongly exchange-coupled and surface-state-modulated magnetization dynamics in $\text{Bi}_2\text{Se}_3/\text{yttrium iron garnet}$ heterostructures, *Nat. Commun.* **9**, 223 (2018).
- [100] D. Zhu, Y. Wang, S. Shi, K.-L. Teo, Y. Wu, and H. Yang, Highly efficient charge-to-spin conversion from in situ $\text{Bi}_2\text{Se}_3/\text{Fe}$ heterostructures, *Appl. Phys. Lett.* **118**, 062403 (2021).
- [101] R. Ramaswamy, T. Dutta, S. Liang, G. Yang, M. S. M. Saifullah, and H. Yang, Spin orbit torque driven magnetization switching with sputtered Bi_2Se_3 spin current source, *J. Phys. D* **52**, 224001 (2019).
- [102] A. Baker, A. Figueroa, L. Collins-McIntyre, G. Van Der Laan, and T. Hesjedal, Spin pumping in ferromagnet-topological insulator-ferromagnet heterostructures, *Sci. Rep.* **5**, 7907 (2015).
- [103] P. Deorani, J. Son, K. Banerjee, N. Koirala, M. Brahlek, S. Oh, and H. Yang, Observation of inverse spin Hall effect in bismuth selenide, *Phys. Rev. B* **90**, 094403 (2014).
- [104] Y. Shiomi, K. Nomura, Y. Kajiwara, K. Eto, M. Novak, K. Segawa, Y. Ando, and E. Saitoh, Spin-electricity conversion induced by spin injection into topological insulators, *Phys. Rev. Lett.* **113**, 196601 (2014).
- [105] H. Wang, J. Kally, J. S. Lee, T. Liu, H. Chang, D. R. Hickey, K. A. Mkhoyan, M. Wu, A. Richardella, and N. Samarth, Surface-state-dominated spin-charge current conversion in topological-insulator-ferromagnetic-insulator heterostructures, *Phys. Rev. Lett.* **117**, 076601 (2016).
- [106] B. B. Singh, S. K. Jena, M. Samanta, K. Biswas, and S. Bedanta, High spin to charge conversion efficiency in electron beam-evaporated topological insulator Bi_2Se_3 , *ACS Appl. Mater. Interfaces* **12**, 53409 (2020).
- [107] Z. Zheng, Y. Zhang, D. Zhu, K. Zhang, X. Feng, Y. He, L. Chen, Z. Zhang, D. Liu, Y. Zhang *et al.*, Perpendicular magnetization switching by large spin-orbit torques from sputtered Bi_2Te_3 , *Chin. Phys. B* **29**, 078505 (2020).
- [108] T. Fan, N. H. D. Khang, S. Nakano, and P. N. Hai, Ultrahigh efficient spin orbit torque magnetization switching in fully sputtered topological insulator and ferromagnet multilayers, *Sci. Rep.* **12**, 2998 (2022).
- [109] Y. Fan, P. Upadhyaya, X. Kou, M. Lang, S. Takei, Z. Wang, J. Tang, L. He, L.-T. Chang, M. Montazeri, G. Yu, W. Jiang, T. Nie, R. N. Schwartz, Y. Tserkovnyak, and K. L. Wang, Magnetization switching through giant spin-orbit torque in a magnetically doped topological insulator heterostructure, *Nat. Mater.* **13**, 699 (2014).
- [110] Y. Fan, X. Kou, P. Upadhyaya, Q. Shao, L. Pan, M. Lang, X. Che, J. Tang, M. Montazeri, K. Murata *et al.*, Electric-field control of spin-orbit torque in a magnetically doped topological insulator, *Nat. Nanotechnol.* **11**, 352 (2016).
- [111] Y. Wang, D. Zhu, Y. Wu, Y. Yang, J. Yu, R. Ramaswamy, R. Mishra, S. Shi, M. Elyasi, K.-L. Teo, Y. Wu, and H. Yang, Room temperature magnetization switching in topological

- insulator-ferromagnet heterostructures by spin-orbit torques, *Nat. Commun.* **8**, 1364 (2017).
- [112] J. Han, A. Richardella, S. A. Siddiqui, J. Finley, N. Samarth, and L. Liu, Room-temperature spin-orbit torque switching induced by a topological insulator, *Phys. Rev. Lett.* **119**, 077702 (2017).
- [113] N. H. D. Khang, Y. Ueda, and P. N. Hai, A conductive topological insulator with large spin Hall effect for ultralow power spin-orbit torque switching, *Nat. Mater.* **17**, 808 (2018).
- [114] M. Dc, R. Grassi, J.-Y. Chen, M. Jamali, D. R. Hickey, D. Zhang, Z. Zhao, H. Li, P. Quarterman, Y. Lv, M. Li, A. Manchon, K. A. Mkhoyan, T. Low, and J.-P. Wang, Room-temperature high spin-orbit torque due to quantum confinement in sputtered $\text{Bi}_x\text{Se}_{(1-x)}$ films, *Nat. Mater.* **17**, 800 (2018).
- [115] T. Gao, A. Qaiumzadeh, R. E. Troncoso, S. Haku, H. An, H. Nakayama, Y. Tazaki, S. Zhang, R. Tu, A. Asami *et al.*, Impact of inherent energy barrier on spin-orbit torques in magnetic-metal/semimetal heterojunctions, *Nat. Commun.* **14**, 5187 (2023).
- [116] J. H. Cullen, R. B. Atencia, and D. Culcer, Spin transfer torques due to the bulk states of topological insulators, *Nanoscale* **15**, 8437 (2023).
- [117] D. Culcer, A. Sekine, and A. H. MacDonald, Interband coherence response to electric fields in crystals: Berry-phase contributions and disorder effects, *Phys. Rev. B* **96**, 035106 (2017).
- [118] See Supplemental Material at <http://link.aps.org/supplemental/10.1103/PhysRevB.108.245418> for a detailed derivation of the spin current and details on the scattering term.
- [119] M. Farokhnezhad, R. Asgari, and D. Culcer, Spin-orbit torques due to extrinsic spin-orbit scattering of topological insulator surface states: Out-of-plane magnetization, *J. Phys. Mater.* **6**, 014002 (2023).
- [120] M. Farokhnezhad, R. Asgari, and D. Culcer, Spin-orbit torques due to warped topological insulator surface states with an in-plane magnetization, [arXiv:2306.12557](https://arxiv.org/abs/2306.12557).
- [121] A. Jash, A. Kumar, S. Ghosh, A. Bharathi, and S. S. Banerjee, Imaging current distribution in a topological insulator Bi_2Se_3 in the presence of competing surface and bulk contributions to conductivity, *Sci. Rep.* **11**, 7445 (2021).
- [122] M. Bianchi, D. Guan, S. Bao, J. Mi, B. B. Iversen, P. D. King, and P. Hofmann, Coexistence of the topological state and a two-dimensional electron gas on the surface of Bi_2Se_3 , *Nat. Commun.* **1**, 128 (2010).
- [123] M. Bahramy, P. King, A. De La Torre, J. Chang, M. Shi, L. Patthey, G. Balakrishnan, P. Hofmann, R. Arita, N. Nagaosa *et al.*, Emergent quantum confinement at topological insulator surfaces, *Nat. Commun.* **3**, 1159 (2012).
- [124] Y. Xia, D. Qian, D. Hsieh, L. Wray, A. Pal, H. Lin, A. Bansil, D. Grauer, Y. S. Hor, R. J. Cava *et al.*, Observation of a large-gap topological-insulator class with a single Dirac cone on the surface, *Nat. Phys.* **5**, 398 (2009).
- [125] H. Liu, R. B. Atencia, N. Medhekar, and D. Culcer, Coherent backscattering in the topological Hall effect, *Mater. Quantum Technol.* **3**, 025002 (2023).
- [126] P. H. Chang, T. Markussen, S. Smidstrup, K. Stokbro, and B. K. Nikolić, Nonequilibrium spin texture within a thin layer below the surface of current-carrying topological insulator Bi_2Se_3 : A first-principles quantum transport study, *Phys. Rev. B* **92**, 201406(R) (2015).
- [127] I. A. Ado, O. A. Tretiakov, and M. Titov, Microscopic theory of spin-orbit torques in two dimensions, *Phys. Rev. B* **95**, 094401 (2017).
- [128] D. Kurebayashi and N. Nagaosa, Theory of current-driven dynamics of spin textures on a surface of topological insulators, *Phys. Rev. B* **100**, 134407 (2019).
- [129] A. Sakai and H. Kohno, Spin torques and charge transport on the surface of topological insulator, *Phys. Rev. B* **89**, 165307 (2014).
- [130] M. H. Fischer, A. Vaezi, A. Manchon, and E. A. Kim, Spin-torque generation in topological insulator based heterostructures, *Phys. Rev. B* **93**, 125303 (2016).
- [131] P. B. Ndiaye, C. A. Akosa, M. H. Fischer, A. Vaezi, E. A. Kim, and A. Manchon, Dirac spin-orbit torques and charge pumping at the surface of topological insulators, *Phys. Rev. B* **96**, 014408 (2017).
- [132] Z. B. Siu, Y. Wang, H. Yang, and M. B. Jalil, Spin accumulation in topological insulator thin films—influence of bulk and topological surface states, *J. Phys. D* **51**, 425301 (2018).
- [133] J. Zhang, J. P. Velev, X. Dang, and E. Y. Tsymlal, Band structure and spin texture of $\text{Bi}_2\text{Be}_3/3d$ ferromagnetic metal interface, *Phys. Rev. B* **94**, 014435 (2016).
- [134] J. M. Marmolejo-Tejada, K. Dolui, P. Lazić, P. H. Chang, S. Smidstrup, D. Stradi, K. Stokbro, and B. K. Nikolić, Proximity band structure and spin textures on both sides of topological-insulator/ferromagnetic-metal interface and their charge transport probes, *Nano Lett.* **17**, 5626 (2017).
- [135] Y. Wang, R. Ramaswamy, and H. Yang, FMR-related phenomena in spintronic devices, *J. Phys. D* **51**, 273002 (2018).
- [136] K. Gupta, R. J. H. Wesselink, R. Liu, Z. Yuan, and P. J. Kelly, Disorder dependence of interface spin memory loss, *Phys. Rev. Lett.* **124**, 087702 (2020).
- [137] K. Dolui and B. K. Nikolić, Spin-memory loss due to spin-orbit coupling at ferromagnet/heavy-metal interfaces: Ab initio spin-density matrix approach, *Phys. Rev. B* **96**, 220403(R) (2017).
- [138] V. K. Dugaev, M. Inglot, E. Y. Sherman, and J. Barnaś, Robust impurity-scattering spin Hall effect in a two-dimensional electron gas, *Phys. Rev. B* **82**, 121310(R) (2010).
- [139] J. R. Bindel, M. Pezzotta, J. Ulrich, M. Liebmann, E. Y. Sherman, and M. Morgenstern, Probing variations of the Rashba spin-orbit coupling at the nanometre scale, *Nat. Phys.* **12**, 920 (2016).
- [140] A. Dyrdal, J. Barnaś, and A. Fert, Spin-momentum-locking inhomogeneities as a source of bilinear magnetoresistance in topological insulators, *Phys. Rev. Lett.* **124**, 046802 (2020).